



Testing the Validity of the Effective Rate Constant Approximation for Surface Reaction with Transport

D. A. EDWARDS* AND S. A. JACKSON†

Department of Mathematical Sciences, University of Delaware
Newark, DE, 19716-2553, U.S.A.

edwards@math.udel.edu

upacific@udel.edu

(Received November 2000; revised and accepted July 2001)

Abstract—When one incorporates transport effects into a surface-volume reaction, an integro-differential equation for the bound state concentration occurs. Such a form is inconvenient for data analysis. An effective rate constant approximation for the solution is correct to $O(Da^2)$ as the Damköhler number $Da \rightarrow 0$. A numerical simulation of the integrodifferential equation is performed which shows that the effective rate constant approximation is useful even outside this regime. © 2002 Elsevier Science Ltd. All rights reserved.

Keywords—Surface-volume reactions, Integrodifferential equations, Numerical simulation, Surface plasmon resonance, BIAcore™.

1. INTRODUCTION

To understand better the chemical reactions that occur inside living organisms, scientists need accurate quantitative measurements of the governing *rate constants* for the reaction. Surface plasmon resonance (SPR) allows the measurement of rate constants in surface-volume reactions such as those that occur on the surface of a cell [1], and the BIAcore™ is a popular device for performing SPR. The BIAcore™ device consists of a channel through which one of the reactants (the *analyte*) is convected in standard two-dimensional Poiseuille flow from $x = 0$, the inlet position. The other reactant, called the receptor, is coupled to a sensor surface on the ceiling of the channel. (See Figure 1.) Reactant binding causes refractive changes in a polarized light beam which are then averaged over the length of the ceiling to provide real-time measurement of the bound-state concentration [2,3]. This data is then transferred to a regression program which predicts the rate constants using a mathematical model.

*Author to whom correspondence should be addressed. This work was supported by the University of Delaware Research Foundation.

†Current address: Federal Sector/Defense Group, Computer Sciences Corporation, Moorestown, NJ 08057-0902, U.S.A.

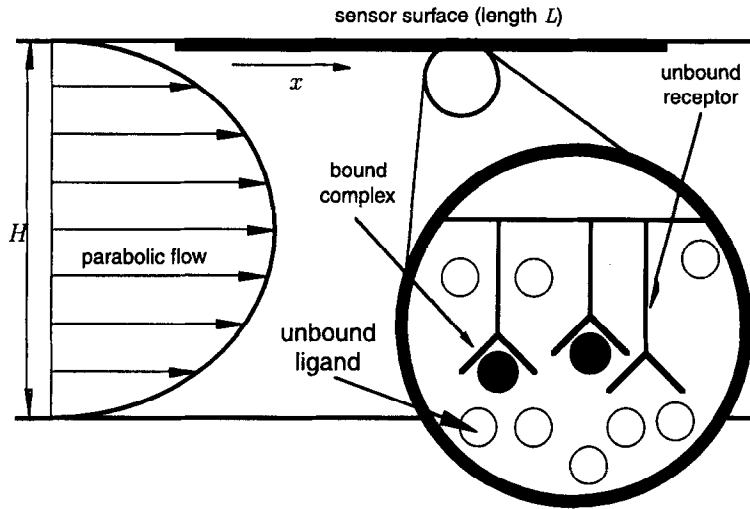


Figure 1. Schematic of BIAcore™ device.

Unfortunately, until recently, these models have treated only the case where the analyte was distributed uniformly along the channel. Thus, transport effects were neglected since the transport was essentially taken to be instantaneous. In this paper, we discuss the complications that arise when transport is taken into account and demonstrate numerically that an approximation formally correct for small transport effects is actually good for a wide parameter range.

2. GOVERNING EQUATIONS

As mentioned above, the simplest case to consider is where transport effects are absent. In this case, the reaction is governed by the simple (dimensionless) ODE

$$\frac{dB}{dt} = (1 - B) - KB, \quad B(0) = 0, \quad (1)$$

where B is the concentration of the bound state and K is the *affinity constant*, which is a ratio of the rate constants [4]. In this case, B is independent of the distance along the channel x and the averaging of the data does not affect the calculation of the rate constants.

However, it can be shown [4] that in the presence of transport effects with large Peclet number (as is achieved in the BIAcore™), the actual governing equation for B is as follows:

$$\frac{\partial B}{\partial t} = [1 - \text{Da}C(x, t)](1 - B) - KB, \quad B(x, 0) = 0; \quad x \in [0, 1], \quad (2a)$$

$$C(x, t) = \frac{1}{3^{1/3}\Gamma(2/3)} \int_0^x \frac{\partial B}{\partial t}(x - \xi, t) \frac{d\xi}{\xi^{2/3}}, \quad (2b)$$

$$\text{Da} = \frac{(\tilde{k}_a R_T L^{1/3} h^{1/3})}{V^{1/3} \tilde{D}^{2/3}} = \frac{\text{reaction rate}}{\text{diffusion rate in unstirred layer}}.$$

Here C represents the deviation of the analyte concentration from the uniform value 1 implicit in equation (1). Note from (2b) that as expected, the analyte depleted at x is an integral of the differential changes upstream ($0 < \xi < x$).

Da is the *Damköhler number*, which measures the strength of transport effects. The “unstirred layer” refers to the boundary layer near the surface of width $\text{Pe}^{-1/3}$ where diffusion and convection balance. In the definition of Da , \tilde{k}_a is the association (“on”) constant, R_T is the total number of sites available for binding, L and h are the dimensions of the channel, V is related to the velocity of the analyte, and \tilde{D} is the diffusion coefficient.

Due to the integral in (2b), system (2) is difficult to solve. Also, it provides solutions for B , not its average, so the solutions thus obtained have to be manipulated again to obtain forms compatible with the data stream. However, if Da is small, equation (2a) suggests a perturbation expansion in that parameter. To leading order, equation (1) holds for B , and thus, the bound state is nearly uniform in x . Because of this leading-order uniformity in B , the average deviation of C from its equilibrium value may be written asymptotically as $F(x)\frac{\partial \bar{B}}{\partial t}$, so the time dependence factors out. Then the leading order of (2b) may be explicitly solved, and the result substituted into (2a). Upon averaging, we obtain [5]

$$\frac{d\bar{B}}{dt} = [(1 - \bar{B}) - K\bar{B}](1 - p) + O(Da^2), \quad p = \frac{Da(1 - \bar{B})\bar{F}}{1 + Da(1 - \bar{B})\bar{F}}. \quad (3)$$

Similar expressions may be obtained for reactions in arbitrary geometries [6].

In (3), \bar{B} is the average of the bound state concentration. Thus, (3) is in a form compatible with the data stream. In a dissociation experiment, p is the probability that an analyte molecule dissociating from the surface will rebind further downstream [5], and here the interpretation is similar. Essentially, p is the probability that an analyte molecule will be unavailable for binding due to inefficient transport. Since \bar{F} is independent of t , it is a function only of the geometry of the system under consideration [6].

Therefore, not only is (3) a more useful form for analysis, it also yields interesting physical interpretations. However, at this stage it has been determined to be useful only in the limit that $Da \rightarrow 0$. Can we extend this result?

3. NUMERICAL SIMULATIONS

Equation (3) has been used in simulations of the binding process in the case where Da is moderate, and has yielded reasonably accurate results [7,8]. We now present the results of a systematic series of simulations where solutions of (2) and (3) are compared to determine the efficacy of (3) when Da is moderate. The algorithm used for (3) was a standard explicit Euler scheme.

The algorithm for (2) is more subtle, reflecting the increased complexity of the problem. First, we note that due to the form of the convolution integral, the value of $C(x, t)$ (and hence, $B(x, t)$) depends only on those values of $B(\xi, t)$ for $\xi \leq x$. Therefore, by solving first at $x = 0$ and working downstream for each time step, we may use *updated* values of $\frac{\partial B}{\partial t}(\xi, t)$ at each grid point. However, the scheme is not fully implicit; for $B(x, t)$ itself, the value from the previous time step was used. This choice, though it makes the method only semi-implicit, rather than fully implicit, forces (4) to reduce to the discretization of (3) when $Da = 0$, thus ensuring consistency in the results.

Indexing space by i and time by n , a schematic version of the algorithm is shown below:

$$\frac{\partial B_{i,n+1}}{\partial t} = (1 - DaC_{i,n+1})(1 - B_{i,n}) - KB_{i,n}, \quad B_{i,0} = 0, \quad (4a)$$

$$C_{i,n+1} = \frac{1}{3^{1/3}\Gamma(2/3)} \int_0^{x_i} \frac{\partial B}{\partial t}(x_i - \xi, t_{n+1}) \frac{d\xi}{\xi^{2/3}}. \quad (4b)$$

One further complication is the $\xi^{-2/3}$ singularity in the convolution integral. This was handled by subtracting out the singularity and then integrating directly. Schematically, the algorithm replacing (4b) was as follows:

$$C_{i,n+1} = \frac{1}{3^{1/3}\Gamma(2/3)} \left\{ \int_0^{x_i} \left[\frac{\partial B}{\partial t}(x_i - \xi, t_{n+1}) - \frac{\partial B_{i,n+1}}{\partial t} \right] \frac{d\xi}{\xi^{2/3}} + 3 \frac{\partial B_{i,n+1}}{\partial t} x_i^{1/3} \right\}. \quad (5)$$

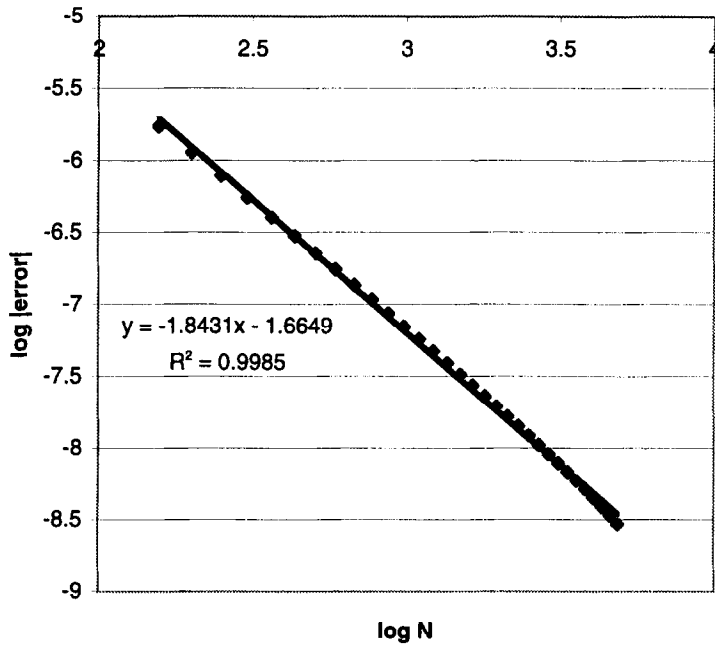


Figure 2. Error of discretized solution. The error plotted is the largest difference between the solution with N grid points and the solution with 80 grid points for a complete run with $Da = 0.45$, $K = 1$.

Note that the integral no longer has a singularity at $\xi = 0$. The numerical integration was performed using the trapezoidal rule.

In the BIAcoreTM, the *scanning range* over which the solution is averaged is not the entire interval. Therefore, the solution once obtained, was averaged using the midpoint rule on a prescribed subset of internal mesh points. Not only does this averaging simulate the actual instrument, but also it makes the numerical simulation more accurate, since the $x^{1/3}$ singularity near $x = 0$ is not considered in the averaging. The simulation ran until one of the derivatives in either (2) or (3) was less than a tolerance based on Δt .

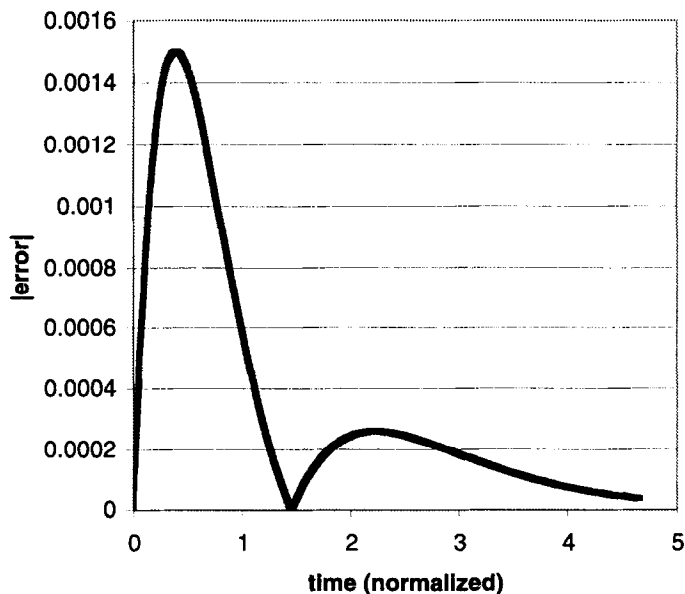


Figure 3. Error between effective rate constant and full numerical solution vs. t for a complete run with $Da = 0.45$, $K = 1$.

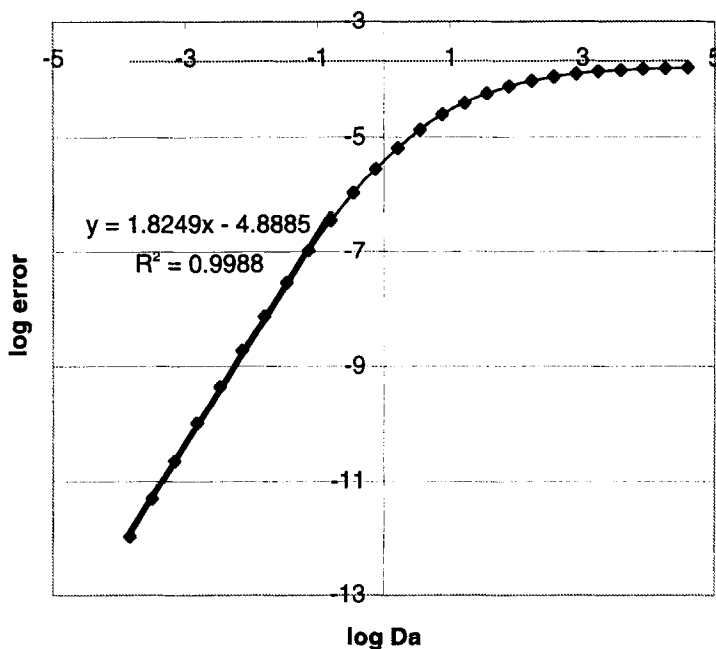


Figure 4. Error between effective rate constant and full numerical solution vs. Da for runs with $K = 1$, $N = 100$.

To test the accuracy of our numerical algorithm (4) and (5), we performed several experiments with differing values of Δx , using the most refined solution as the baseline. The results are shown in Figure 2. The discretization error shown (the largest for an entire simulation) compares favorably with the estimate of $(\Delta x)^{5/3}$ obtained by using simpler test cases. (The reduction of accuracy from the normal $(\Delta x)^2$ in the trapezoidal rule is a result of the singularity in the convolution integral.) Therefore, we always set our time step equal to $(\Delta x)^2$ to ensure that spatial discretization error dominated.

To compare the accuracy of the effective rate constant solution, we graphed the error between the numerical solutions of (2) and (3) throughout an experiment. The results are shown in Figure 3. As one can see, the error is quite small even though Da is moderate.

Last, we tested the main hypothesis: whether the effective rate constant equation can be used successfully outside the parameter range where it was derived. An experiment was designed with $\Delta x = 0.01$, which corresponds to a discretization error of 4×10^{-4} . The results are shown in Figure 4. Note that for small Da , the error (again the largest for an entire simulation) grows like Da^2 , as predicted. Then as Da increases, the error remains small, eventually approaching a maximum value as $Da \rightarrow \infty$. This is because as $Da \rightarrow \infty$, $p \rightarrow 1$ and we eventually reach a case where the transport is so slow that the downstream sites are starved for analyte. However, this asymptote is still small (corresponding to roughly a 2% error), and thus, we see that the effective rate constant solution provides a good estimate to the solution even when Da is not small, especially when one considers that there will be noise in any laboratory experiment.

4. CONCLUSIONS AND FURTHER RESEARCH

Given the current state of the art in SPR technology, simple models for surface-volume reactions are needed to obtain accurate constants for the reactions. Though the full model for such a reaction in the BIAcoreTM consists of an integrodifferential equation, the effective rate constant solution can be shown to be a good approximation to the true solution when $Da \rightarrow 0$. With the results presented here, we have now shown numerically that when transport effects play a significant role, the effective rate constant approximation still provides useful rate constant estimates.

Further research will use more sophisticated algorithms to compute the solution, as well as take into account other physical effects in the BIAcoreTM, such as the fact that the reaction does not always take place on a surface, but rather in a thin dextran layer adhered to the channel ceiling.

REFERENCES

1. B. Goldstein and M. Dembo, Approximating the effects of diffusion on reversible reactions at the cell surface: Ligand-receptor kinetics, *Biophys. J.* **68**, 1222–1230, (1995).
2. R. Karlsson, A. Michaelson and L. Mattson, Kinetic analysis of monoclonal antibody-antigen interactions with a new biosensor based analytical system, *J. Immun. Meth.* **145**, 229–240, (1991).
3. A. Szabo, L. Stolz and R. Granzow, Surface plasmon resonance and its use in biomolecular interaction analysis (BIA), *Curr. Opin. Struct. Bio.* **5**, 699–705, (1995).
4. D.A. Edwards, Estimating rate constants in a convection-diffusion system with a boundary reaction, *IMA J. Appl. Math.* **63**, 89–112, (1999).
5. D.A. Edwards, B. Goldstein and D.S. Cohen, Transport effects on surface-volume biological reactions, *J. Math. Bio.* **39**, 533–561, (1999).
6. D.A. Edwards, Biochemical reactions on helical structures, *SIAM J. Appl. Math.* **60**, 1425–1446, (2000).
7. T. Mason, A.R. Pineda, C. Wofsy and B. Goldstein, Effective rate models for the analysis of transport-dependent biosensor data, *Math. Biosci.* **159**, 123–144, (1999).
8. D.G. Myszka, X. He, M. Dembo, T.A. Morton and B. Goldstein, Extending the range of rate constants available from BIAcoreTM: Interpreting mass transport influenced binding data, *Biophys. J.* **75**, 583–594, (1998).